

Sensorimotor: P.M. Synchronous Motor With Fully Integrated Position Sensor

INTRODUCTION

Historically, the machine design and process engineer applying motion control systems has been confronted with the choice of using open loop stepping motors or closed loop brush or brushless servo systems. In certain applications, brush motor systems are simply not viable due to maintenance and environmental constraints. His perception tends to be that servos are costly and cumbersome but offer a performance advantage while steppers are “simple” and more cost-effective, yet also have inherent performance limitations.

Integrated Engineering Software - Website Links

[Home](#)[Products](#)[Support](#)[Technical Papers](#)

"Page Down" or use scroll bars to read the article



Sensorimotor: P.M. Synchronous Motor
With Fully Integrated Position Sensor
Ralph Horber
Sieberco, Incorporated, 60 Brooks Drive, Braintree, MA 02184

Introduction

Historically, the machine design and process engineer applying motion control systems has been confronted with the choice of using open loop stepping motors or closed loop brush or brushless servo systems. In certain applications, brush motor systems are simply not viable due to maintenance and environmental constraints. His perception tends to be that servos are costly and cumbersome but offer a performance advantage while steppers are "simple" and more cost-effective, yet also have inherent performance limitations.

The primary reason BLDC (AC) servos are considered costly and cumbersome is that they require feedback systems for commutating the motor and closing the position and velocity loops. More often than not, those subcomponents are manufactured by different entities, occasionally leaving the user with assembly and responsibility problems.

In 1985, I co-founded Sieberco (Venture Capital backed) and the Sensorimotor was developed, specifically created to combine the performance advantage of the servo with the cost and mechanical simplicity of the stepper. This was accomplished by integrating the position feedback into the magnetic motor structure. (U.S. Patent No. 4,687,961; patents pending in Japan and Europe.)

The second problem for the machine designer is the choice among a multitude of profile generators or indexers. This device is the link between the motor power section and the higher level machine functions and/or a human operator. Since many indexers are hardware-oriented, they tend to have limited capabilities and be inflexible. Most software indexers also are characterized by their own particularly cryptic commandset, requiring the user to spend a considerable amount of time learning it. To address this problem, we have taken a concept of integration to the indexer level as well, using a 16-bit microcontroller and designing powerful, flexible and user-friendly interface software for utilization with it (explored in greater detail in the application section of this paper).

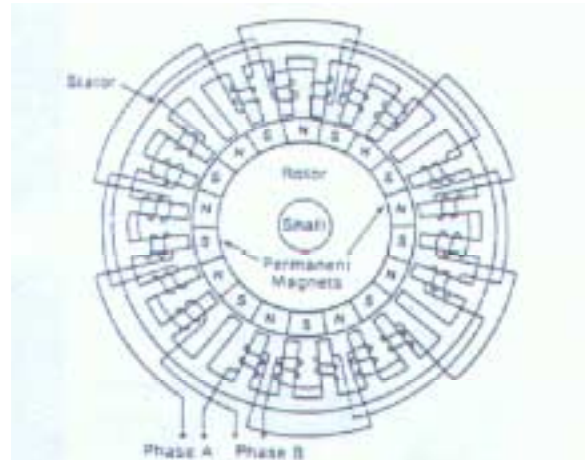


Figure 1. Mechanical construction showing rotor/stator pole relationship and phase windings.

The Motor

The Sensorimotor is a brushless 2-phase, permanent magnet synchronous motor. (Since the motor is driven with a sinusoidal current wave form, some people refer to it as an AC motor.) The stator has 24 salient poles, individually wound as shown in Figure 1. The rotor carries 18 hard magnetic magnets, (SmCo, or Nd-Fe-B), therefore, the motor has 9 electrical cycles per mechanical revolution compared to the typical hybrid stepper with 50 electrical cycles and the typical BLDC with 2 to 4 cycles per revolutions. Figure 1 shows the rotor in the 90% maximum torque position for Phase B, while Phase A is in stable equilibrium.

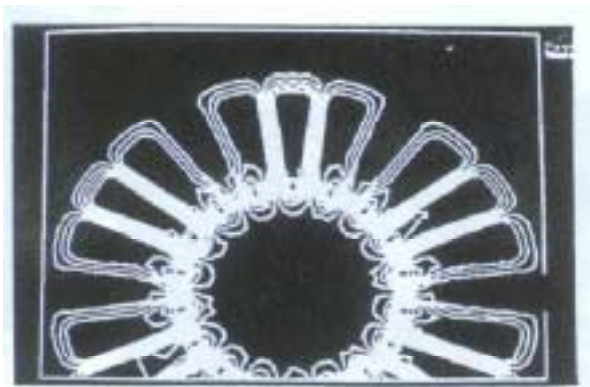


Figure 2. Macrostructure flux pattern.

The magnetic macrostructure (stator flux pattern due to PM-MMF – Figure 2) indicates three diagonal axes of symmetry, dividing the motor into six elementary “motors operating in series.” Therefore, the motor can be completely evaluated by the analysis of the torque components acting on four consecutive stator poles. This plot was made using a Linear Finite Element Analysis Program. As in other PM BLDC motors, as well as in hybrid steppers the cogging or detent torque on the shaft is the sum of the elementary torque components (P1 – P4) due to PM’s only. They tend to be quite high and need to be meticulously balanced. The periodicity of those components is twice the frequency of the electrical cycles since the direction of the torque is a function of the absolute flux in the airgap. The torques for P1– P4 are indicated in Figure 3. The magnitude is approximately seven times the rated output torque of the motor.

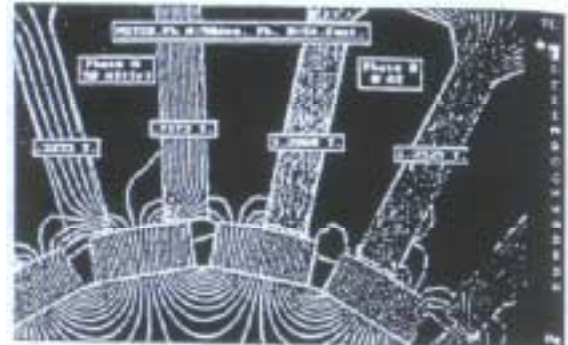


Figure 5. Flux at 50 AT phase current

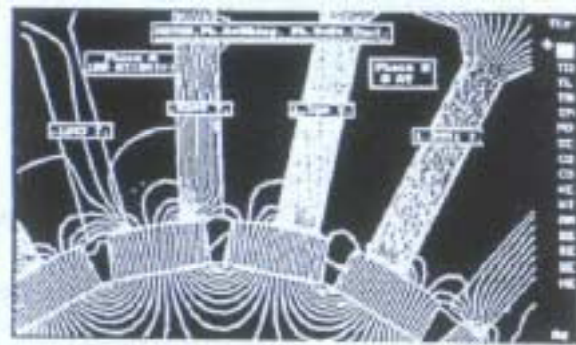


Figure 6. Flux at 100 AT phase current.

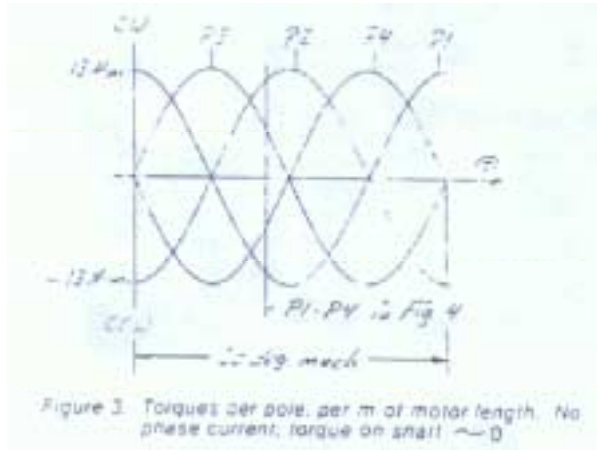


Figure 3. Torques per pole, per m of motor length. No phase current, torque on shaft ~ 0

The following fluxplots (equipotential line plots) were made by the Magneto program, a non-linear, finite boundary element software package manufactured by Integrated Engineering Software. Figures 4, 5, and 6 show the motor in the 90° torque position for Phase A;

the accompanying torques for the four poles are given in Figure 7. As is evident, the coil MMF is used merely to change the balance of the torques due to the PM MMF.

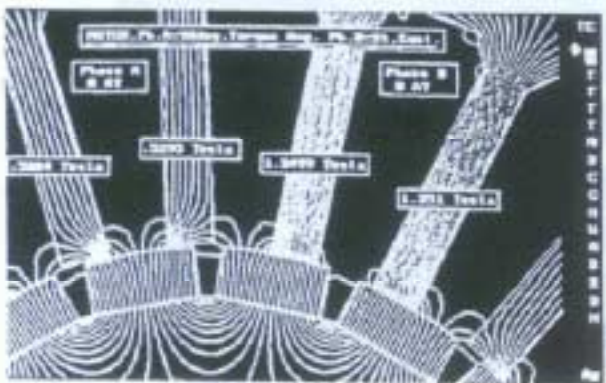


Figure 4. Flux at 0 AT.

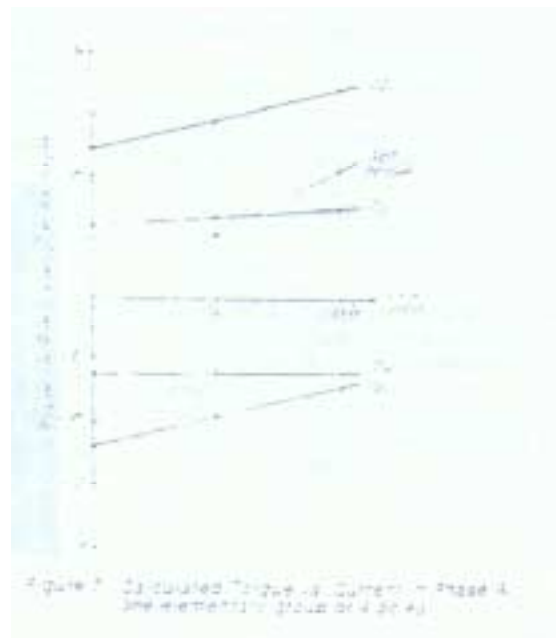


Figure 7. Calculated Torque vs. Current - Phase A. (The elementary group of 4 poles)

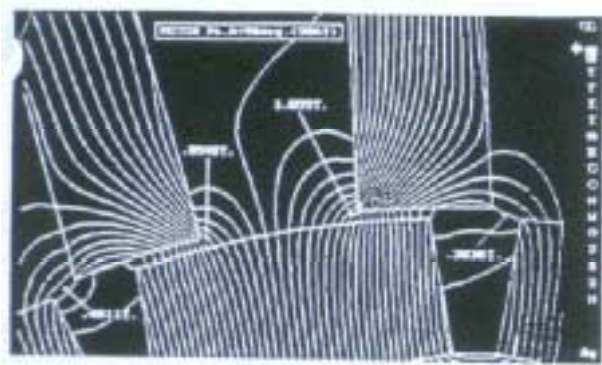


Figure 8 50 AT phase current.

Figure 8 is a zoom-in on P1 and P2 excited on 50 AT. As the flux lines and levels indicate, the torque acting on P1, for example, can be further broken down into CW and CCW torque components. In Figure 7, they have been lumped into one torque acting on P1. The torque vs. current curve is quite linear since Samarium Cobalt has a permeability of approximately 1. On very high coil excitations (10 times

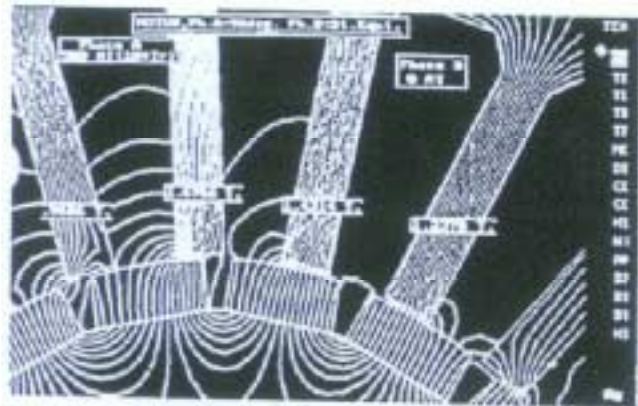


Figure 9. 500 AT phase current.

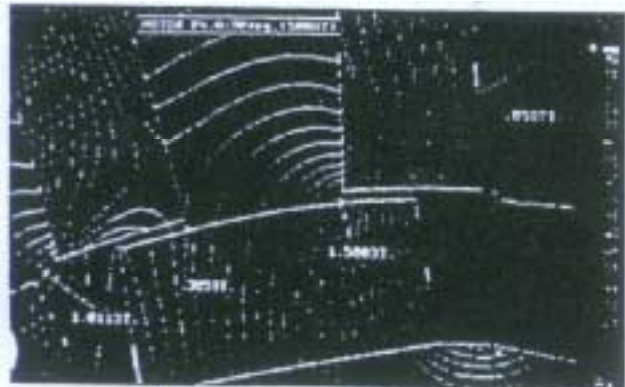


Figure 10 Close-up 500 AT

rated current – Figure 8), leakage on P1 and saturation on P2 occurs. Figure 9 is a closeup of P1 and P2. On P1, the intersection of the PM and coil field having the same polarity can be readily observed indicating a reversal of direction in torque since the CCW component became

dominant. The torques are:

$$P1 = -6.8146 \text{ Nm}$$

$$P2 = -26.632 \text{ Nm}$$

$$P3 = -9.301 \text{ Nm}$$

$$P4 = 6.2112 \text{ Nm}$$

The sum = -36.536 Nm indicating a 28% saturation level. On the actual motor, torque is linear to approximately 5 x Ir. Decreases by 8% on 7 x Ir and 30% on 10 x Ir.

Figures 11 through 15 are flux plots where Phase A is in the 45 deg. Elec. And Phase B is the 135 deg. elec. Position. The motor is sinusoidally driven, so the phases are energized by the $\sqrt{2}$ of current. Figure 16 gives the torques for the four poles on the different excitation levels. Again the torque reversal (P3) can be observed.

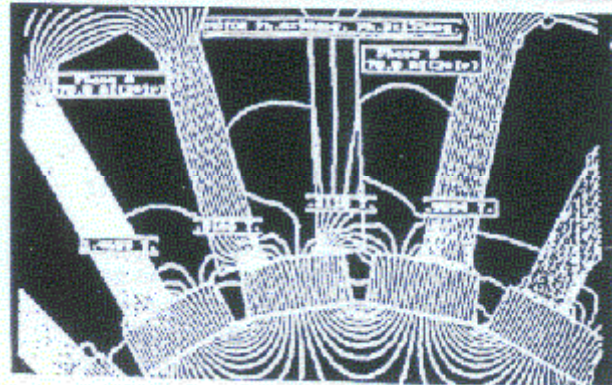
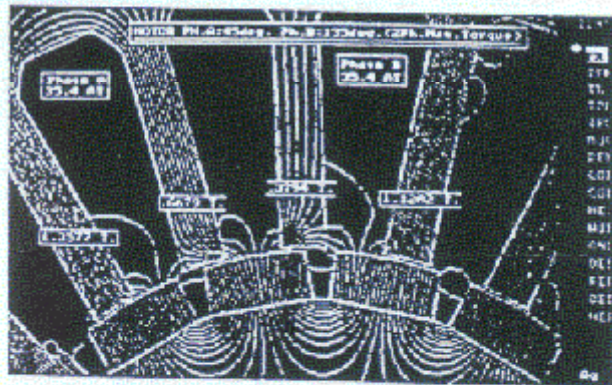
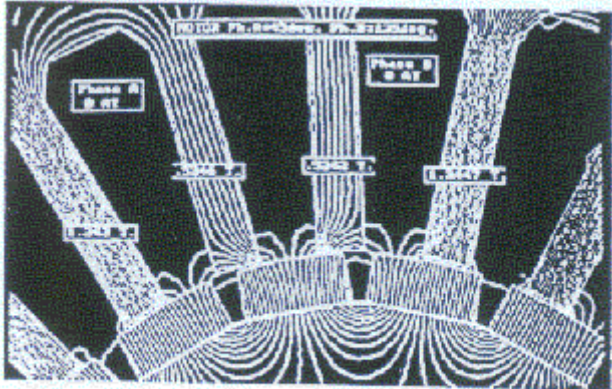


Figure 11 - 13.

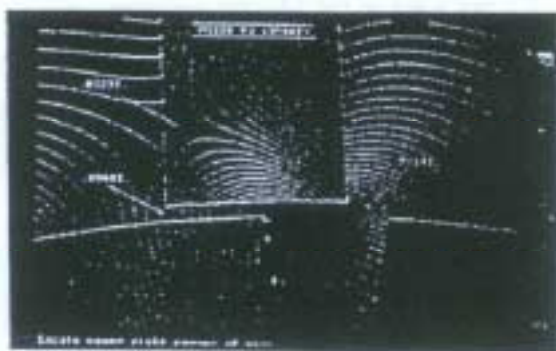


Figure 15.

	θ_1	θ_2	θ_3	θ_4	θ_{ave}
θ_{ave}	-1.027	-1.027	-1.027	-1.027	-1.027
θ_{ave}	-1.027	-1.027	-1.027	-1.027	-1.027
θ_{ave}	-1.027	-1.027	-1.027	-1.027	-1.027
θ_{ave}	-1.027	-1.027	-1.027	-1.027	-1.027

Figure 16. Calculated torques on P1 - P4 in N.m/m.

The Sensor

The mechanism of sensing the rotor position follows well-established principles¹²³. In all reluctance and some PM synchronous machines, the phase inductance varies with rotor position. This is utilized quite often to calculate torque by means of the Co-energy method. The concept is also used in TV and radio electronics when magnetically biased reactors are used in tuned circuits. Figure 17 shows a typical magnetization curve, (PM supplied MMF), Figure 18 shows the electrical sensor arrangement for the sine. The two sensor coils are excited with a 90kHz AC. If the inductance of the two coils is equal, the AC voltage on the CP is half the applied voltage. The rotor magnets provide the magnetic bias thereby reducing the inductance of the coil on the pole facing the rotor magnet. The peak to peak AC voltage on the

CP is at a maximum. This AC is fed into a demodulation circuit where it is rectified to form a DC voltage indicative of the difference in inductance (rotor position) in the two coils.

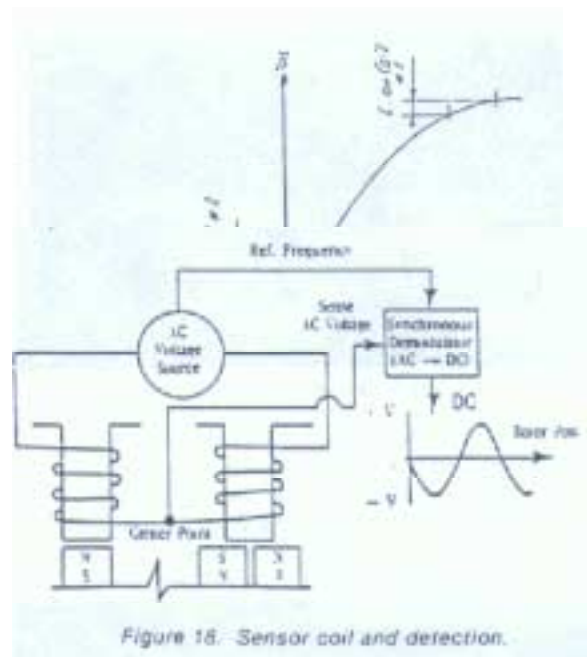


Figure 18. Sensor coil and detection.

The inductance on one coil varies between 270 mH and 610 mH, depending on how much flux from the SmCo magnet links the pole (rotor position). The cosine is formed the same way, but with the two poles magnetically shifted by 90° from the first two poles. The signal magnitude is approximately 5V with a 12V peak to peak applied AC voltage. Figure 19 shows the actual rotor position feedback as it is fed into the microcontroller.

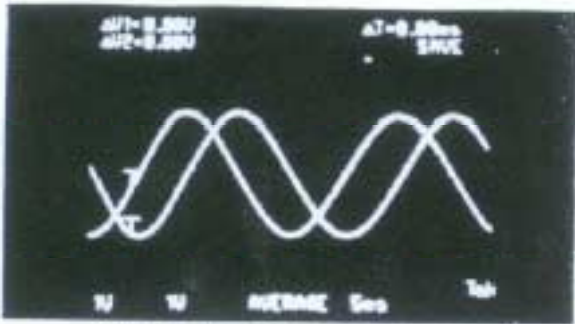


Figure 19. Feedback sine and cosine

Figures 20 – 24 show the PM flux linking poles 1 and 3 to provide the sine and poles 2 and 4 for the cosine. The actual distribution of the sensor poles is according to Figure 1; they are magnetically equivalent to P1 – P4 and are shown consecutively for convenience. Figures 20 – 24 cover 45 electrical degrees as indicated in 25, thereby allowing the reconstruction of the whole cycle.

As can be appreciated, this feedback method has both advantages and disadvantages when compared to others. On the plus side:

- Very robust in adverse environments (physically as well as electrically)
- Temperature insensitive
- Accurate to 10 arc-minutes
- Insensitive to mechanical variation
- 18 cycles per revolution
- Is always aligned properly with the motor
- Manageable data rates
- Low cost
- Phase commutation as well as positioning

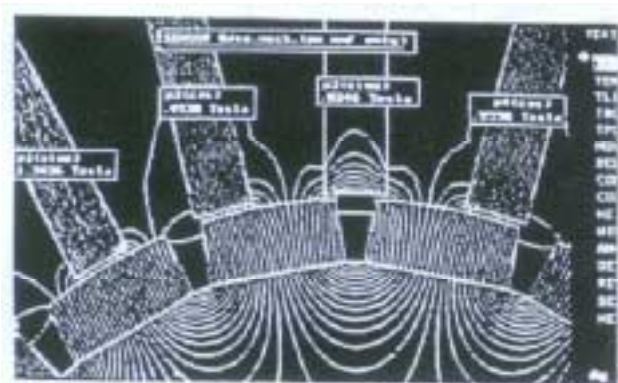


Figure 20. Flux in sensor poles.

On the minus side:

- PM MMF distribution must be accurate (balanced magnets, magnets must be placed equidistantly around the rotor)
- Sensor has twice the electrical cycle count of the motor (must be delay with in the Micro)

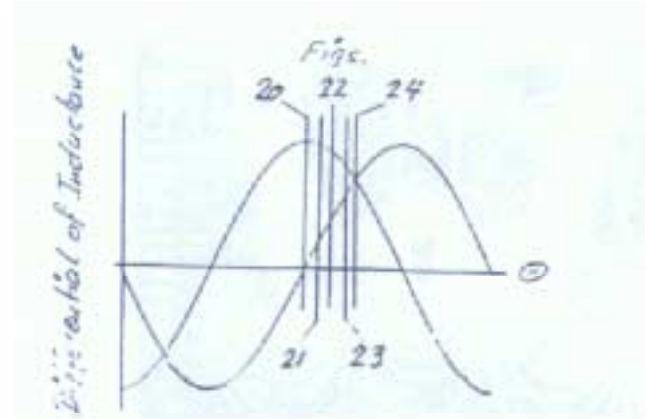


Figure 25. Inductance variation vs. position.

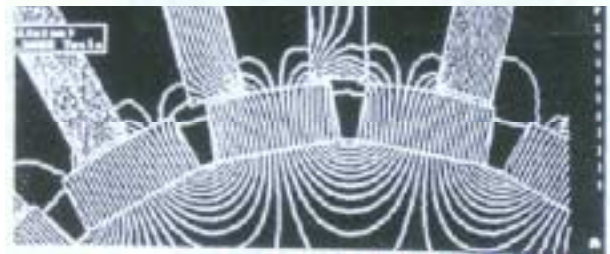


Figure 22. Flux in sensor poles.

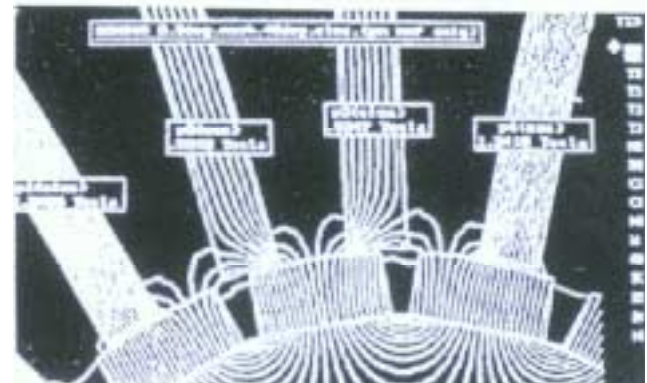
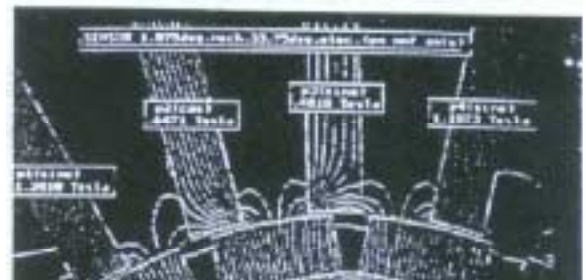


Figure 24. Flux in sensor poles.

Some Aspects of Motor and Sensor Integration

As is evident, the stator/rotor pole combination is crucial in that the relationship of poles must be such that the sine and cosine on the sensor can be accomplished without efficient motor operation being impaired. Also, using four stator poles for sensing purposes cannot disturb the torque balance of the two phases. As can be seen in Figure 1, for the sine feedback, one stator pole from Phase A and one stator pole from Phase B are used. The same is true for the cosine feedback. Furthermore, the balance of torque is maintained by the phase current providing an equal net torque by increasing positive torque and decreasing negative torque. It's shown in Figure 7 and figure 16. To my knowledge, the stator/rotor pole combination of 4/3 (or multiples thereof) is the only one which maintains this balance.

The electrical cycle count of 9 on the motor and 18 on the sensor gives a high torque constant with a broad band (1800 RPM to 2800 RPM) over which 90% of motor power is available. On the sensor, it results in good resolution and accuracy on data rates comensurate with digital commutation and phase advance.

Another aspect is interference from phase current and chopping noise. The demodulation circuit of the sensor rejects all frequency components other than its own and has proven to be very robust in this as well as other situations. However, attention was paid to make sure that subharmonics of the chopping frequency and sensor excitation do not coincide. The influence of large phase currents on sensor pole flux levels is less than 10% due to using load lines greater than 2 on the rotor magnets. Moreover, it is predictable and therefore can be compensated in the Microprocessor. Since the sensor consists of coils that passing of the rotor magnets induces a back EMF in them. This has been counteracted by placing 4 blocking capacitors in the appropriate areas. These are the only electronic components on the motor.

System Software, Interface and Applications

The software is broken into two aspects – Realtime and User Interface. In the Realtime portion, the two feedback signals are captured and processed. The resulting position is used in conjunction with phase advance to commutate the motor via a corrected sin/cosine lockup table. This happens on a sample time of 300 microseconds. The position error which is fed into the PID loop which operates on 900

microseconds. The PID output sets the command torque in the commutation loop. The profile generator or indexer runs concurrent with the PID loop.

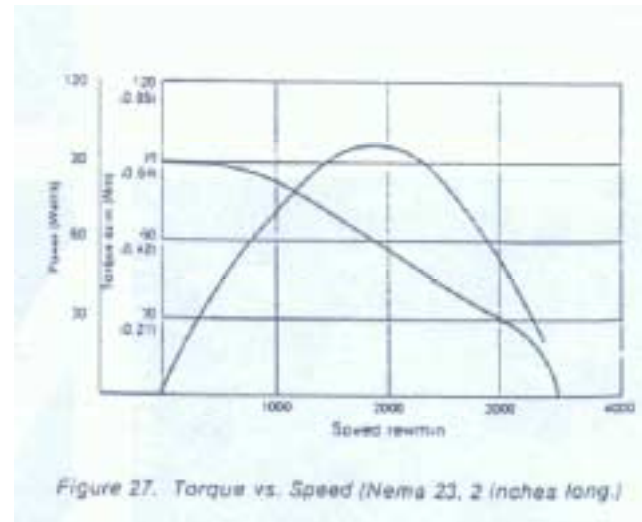
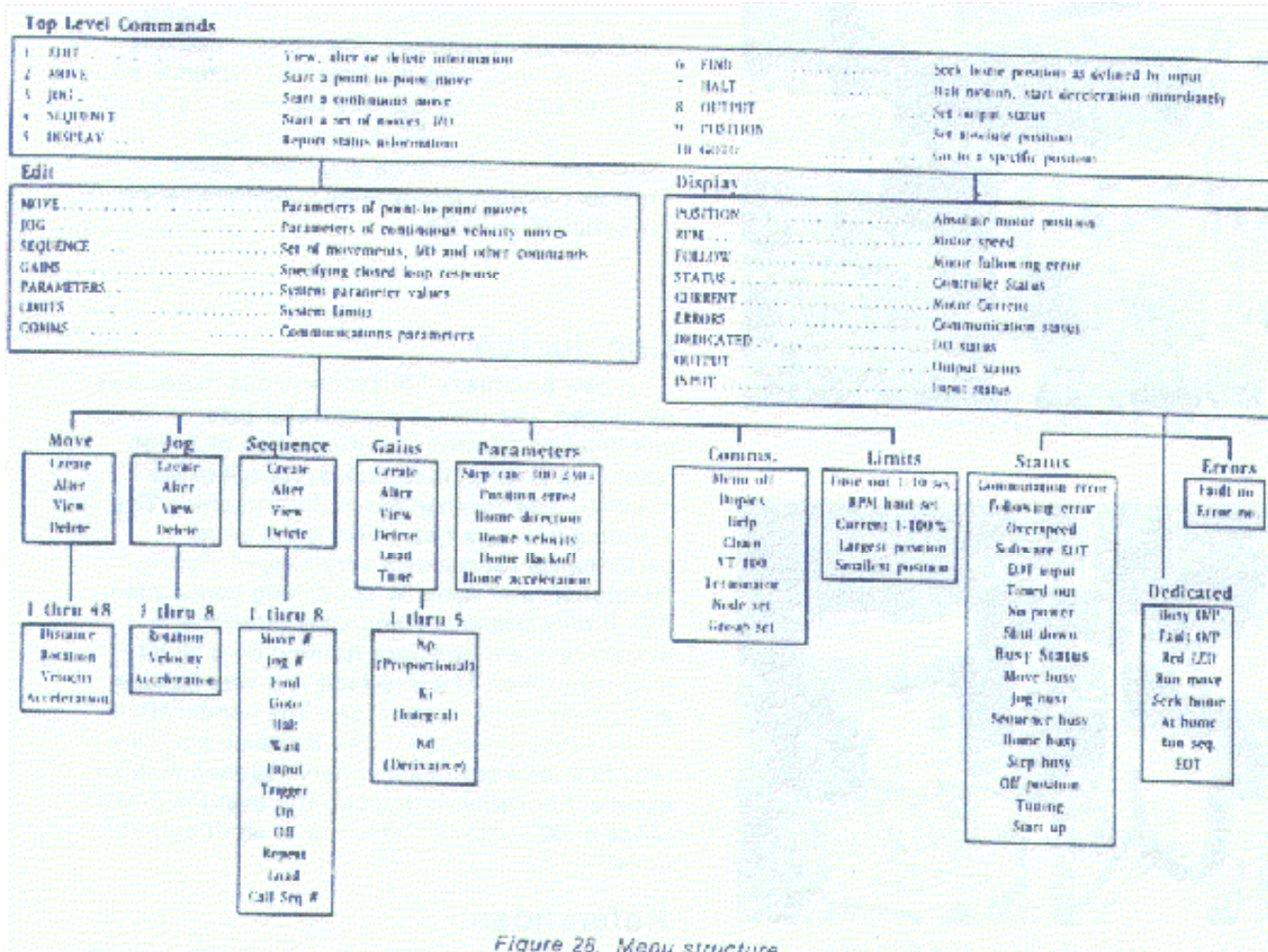
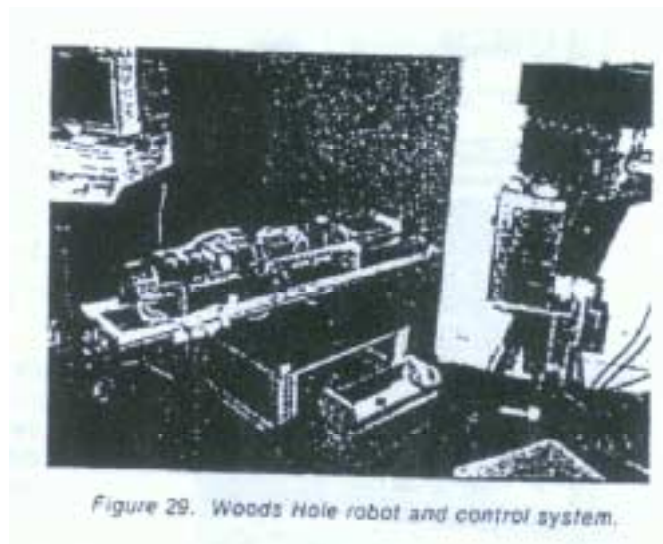


Figure 27. Torque vs. Speed (Nema 23, 2 inches long.)



The User Interface is an English Language Menu structure that is straight forward and easy to operate (Figure 28). The system can be used stand alone, with a PC through serial or parallel communication or with a PLC and discrete I/O. Some applications illustrating the interfaces follow:

- Woods Hole Oceanographic Institute built a miniature Deep Sea Submarine (Used in discovery of the Titanic, Bismark, Black Smokers, etc.). The robotic manipulator on the sub uses sensorimotors, among other things, because the motors must operate under severe oil pressure (10,000 psi). Each of the motor's controllers is addressed parallel through dual port ram. Controllers can be switched from local PID to torque mode. Data from the ship to the submarine and vice versa is through Fiberoptics (Figure 29).
- The Assembly/Packaging of the Cray CPU. Ten Seiberco systems operate in conjunction with two Seiko robots. Some of the systems are addressed through discrete I/O from a PLC, others operate interlinked with each other using Seiberco resident sequences (moves, inputs, etc. – Figure 30 and 31).



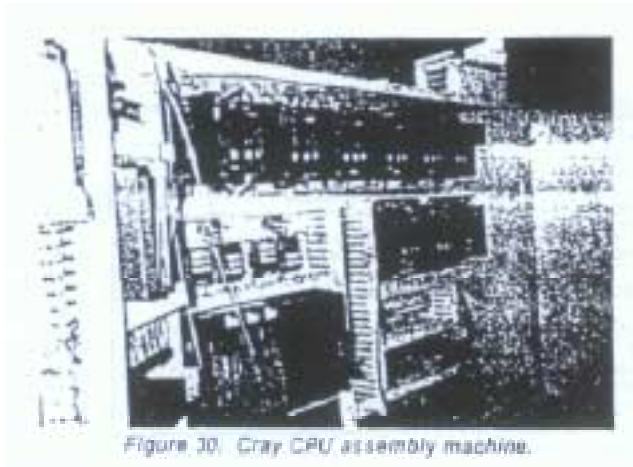


Figure 30. Cray CPU assembly machine.

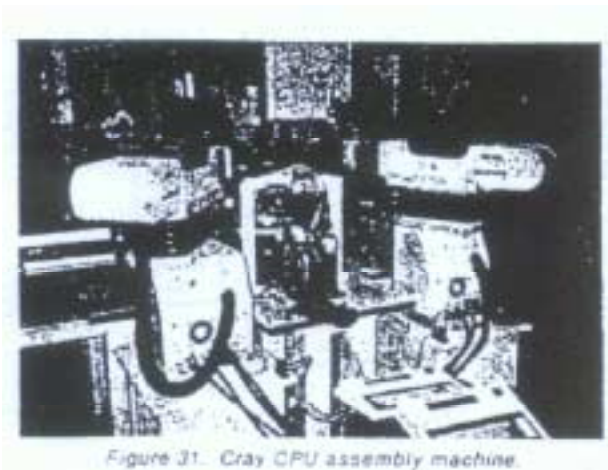


Figure 31. Cray CPU assembly machine.

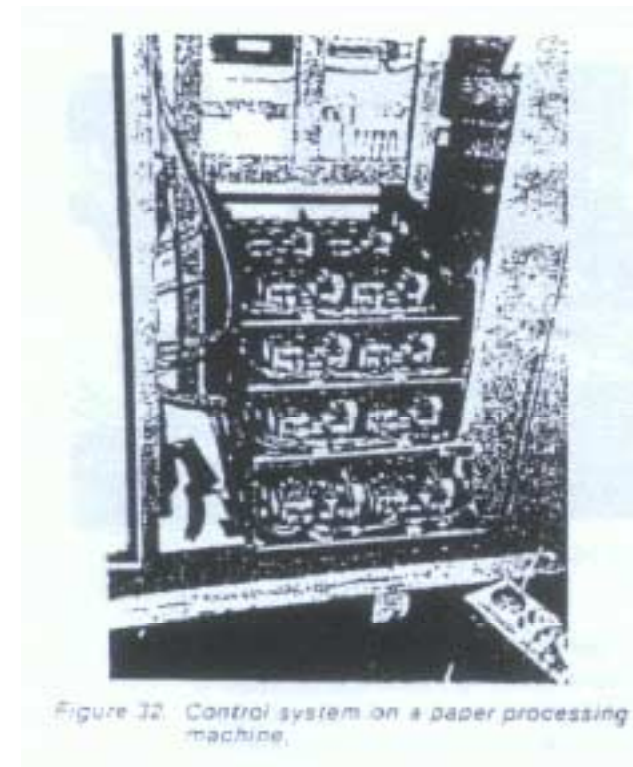


Figure 32. Control system on a paper processing machine.

- A packaging machine uses 16 sensorimotor systems to position side carriers. The control architecture is two-fold. The overall machine functions, including the Seiberco systems, are controlled through discrete I/O from a large PLC. In addition, a PC is used for Operator Interface and to change and query Seiberco resident motion information. Communication is serial. (Figure 32)

Conclusion

A new brushless PM synchronous motor was developed. The unique stator/rotor pole combination allowed the integration of a high resolution position feedback system into the magnetic and mechanical motor structure. The resulting package has a very good price/performance ratio and is very rugged. Further integration was done by combining comutation, PID, profile Generator and User Interface in system resident software running on a 16 bit microcontroller. The interface is a very flexible and powerful menu structure. The combination of the sensorimotor with the Seiberco software results in an easy-to-apply servo system with an excellent price/performance ratio over the power range of 50 watts to 750 watts fo shaft output power.

References:

1. Electromechanics Second Edition S.A. Naser and L.E. Unnewher
2. Electronic Machinery Fourth Edition McGraw Hill
3. Physik Baud II Kurzausgabe Dummler Verlag, West Germany
4. Die elektronischen Grundlagen der Radio-und Fernsehtechnik II. Auflage, Franzis Verland, Kurt Leucht
5. Influencing Fundamental Torque Components in Hybrid Stepping Motors IMCSD 1985, R. Horber

(My special thanks to Albert Leeuhauts whose support was pivotal in the development of the sensorimotor and Professor Hi-Dong Chai whose many papers increased my understanding of magnetics substantially.)